Center of Mass Estimation in Closed Vortices: A Verification in Principle and Practice

STANFORD B. HOOKER AND DONALD B. OLSON

Rosenstiel School of Marine and Atmospheric Science, University of Miami, Department of Meteorology and Physical Oceanography, Miami, FL 33149

(Manuscript received 19 October 1983, in final form 20 April 1984)

ABSTRACT

The problem of tracking closed mesoscale vortices using center of mass estimation techniques is studied. Three estimators are evaluated using data from a warm core Gulf Stream ring. The comparisons show that a method based on the intersection of perpendicular bisectors and one using a least-squares fit of a conic section perform comparably. The perpendicular bisector algorithm is used in conjunction with a Gaussian ring model and a star-shaped survey pattern to produce an expected error curve as a function of vortex translation, survey speed and vortex size. For typical ring parameters, center estimation is usually possible to within ±5 km. The feasibility of using differing data sets to construct a history of ring motion based on a coordinate system moving with the ring is also investigated. In this way, the validity of using satellite-derived data and drifter trajectories to estimate the center of mass of a mesoscale feature is assessed. The results of the analysis demonstrate that the location of the deeper structure of the ring and the surface expression are sufficiently well correlated to permit dynamically relevant calculations based on surface measurements. It is shown that satellite-derived data can be used to approximate the center of mass trajectory to within the error in the individual center estimates for the period analyzed. The Lagrangian-drifter-derived centers are offset from the center of mass trajectory in a manner consistent with kinematic arguments.

1. Introduction

The importance of synoptic scale eddies is well established in the atmosphere, since regional weather is, to a great extent, controlled by these intense disturbances. The circulations and energetics of many oceanic areas, such as the Gulf of Mexico (Elliott, 1982) and the Northwestern Sargasso Sea (The Ring Group, 1981), are also seen to be dominated by large-scale eddies. In addition to these scientific inquiries, the passage of major high- and low-pressure systems in the atmosphere and ocean are followed closely for economic reasons. Considerable effort is expended on accurately tracking tropical cyclones, for instance, due to their potential threat to mariners and coastal regions. Similarly, oceanic eddies have a significant impact upon fisheries, transportation and mineral exploration activities. Summaries of atmospheric cyclone trajectories are compiled and cataloged on a regular basis in journals such as *Monthly Weather Review* and *Mariners Weather Log*. A record of the distribution and motion of oceanic eddies can be found in *Oceanographic Monthly Review*.

In order to study problems concerning the dynamics of eddies, it is necessary to determine their center. In practice, the center can be defined as the center of mass or as the center of circulation. To some extent, the appropriate manner in which to estimate the center of a feature depends upon the particular property of the eddy for which a mean location is wanted, which, in turn, demands a representative contour of the desired property. Since eddies are evolving features, there is the additional constraint that the data be collected synoptically.

Centers determined from different properties are, in general, at different locations in space. The center of mass, for example, is not at the same location as the center of the momentum or energy fields (Smith and Reid, 1982). Nor is the center of a vortex necessarily the point with extremal properties in some variable, even in the ideal case where such a position can be found in the presence of observational and environmental noise. Thus, the center of mass need not coincide with the location of the largest density anomaly.

A trajectory of an eddy's center is of interest in studies of vortex motion and is often used to composite data into a coordinate system moving with the feature. Examples of hurricane translation studies and evaluation of mean tropical storm structure can be found in Chan and Gray (1982) and Willoughby and Chelmow (1982). Olson (1980) used center of mass estimates for a cyclonic Gulf Stream ring to monitor the translation and shape of the feature over time and to calculate the velocity, vorticity and energy fields. The mean structure of small mesoscale oceanic lenses (McDowell and Rossby, 1978; Elliott and Sanford, 1983; Riser *et al.*, 1983) has also been determined using a similar type of analysis.

Many of the previous studies concerning center

estimation assume a specific model for the structure of the eddy—most commonly a circular vortex is assumed. This assumption is explicit in Henrick *et al.* (1979), Riser *et al.* (1983) and Elliott and Sanford (1983), and is implicitly made in the hurricane circulation center estimator dicussed by Willoughby and Chelmow (1982). Although most vortices in the ocean or atmosphere are nearly circular, the bias involved in the symmetric assumption can be avoided easily. In what follows, three estimators are discussed: two are general estimators making no assumption about vortex shape, and the other is based on the vortex having the form of a closed conic section (Brown *et al.*, 1983).

This study makes use of data collected as part of a multidisciplinary oceanographic program known as the Warm Core Rings Experiment (WCRE). A variety of observational platforms were used during the field portion of the WCRE to study the biological, chemical and physical properties of several warm core rings in the North American Slope Water. A warm core ring is composed of a core of Sargasso Sea water encircled by an anticyclonic current of Gulf Stream water, the so-called high velocity region. The outer edge of the high velocity region is the boundary between the ring and its surrounding environment. As such, its surface manifestation is seen as a zone of strong thermal contrast modulated by fluctuations in the frontal boundary. The fluctuations are frequently strong advective features or streamers (Brown, *et al.*, 1983) that can introduce neighboring fluid into the ring.

Of primary interest to all of the scientists involved in the WCRE was determination of the motion and configuration of the ring under investigation over time, not only for the immediate benefit of placing experiments within the eddy field in their proper orientation, but also for constructing a detailed history of ring center location and shape. The latter is perhaps the more important, since it permits ancillary data to be studied in a cylindrical coordinate system moving with the ring, which is its more natural context.

In terms of ring motion, it is most useful to follow the center of mass, since it is the response of the mass field to the applied forcing that determines the translation. The appropriate property to use with center of mass computations is the density, but density is difficult to measure synoptically. The thermal field is a reasonable approximation of the mass field, and it can be surveyed rather quickly using XBTs and star-shaped sampling patterns to construct an Eulerian description of ring translation (Olson and Spence, 1978).

There remains the difficulty of choosing the appropriate isotherm and deciding at what depth level to estimate ring center. Typically, a thermocline level isotherm is used. There are several practical benefits to restricting the analysis to thermocline level isotherms: 1) straightforward linear interpolation can be used to determine the location of the desired isotherm, 2) the thermocline can usually be reached by XBT probes even in the most intense circulations and 3) the thermocline depth is a good predictor for the pressure field in rings whose baroclinic field can be approximated by a two-layer system.

In most surveying programs, ships alone are not sufficient for constructing a long time series of ring position, and other synoptic data sources must be used in conjunction with hydrographic surveys for the purpose of tracking rings.

Drifters have proved useful in determining the evolution of oceanic eddies. In fact, satellite-tracked drifters were instrumental in discovering the ultimate fate of Gulf Stream rings—reabsorption by the Gulf Stream (Richardson, 1980). Drifters are Lagrangian instruments and some care must be taken when using them to augment an Eulerian data set. One of the important lessons of the kinematic models (Flierl, 1981) is that the center of a ring varies with the instrument, Eulerian or Lagrangian, from which center estimates are made, as shown in Fig. 1. The difference is inversely proportional to wave steepness u_o/c, where c is the translation velocity of the vortex and u_o is its swirl velocity, and is a consequence of the Doppler shift $c - u_o$, induced by the translation of the feature. The displacement is greatest when c is large, or u_o is comparatively small (possible with old rings), and zero when the ring is not moving. The displacement direction depends on the rotation of the feature; for an anticyclonic (cyclonic) ring it is toward the south

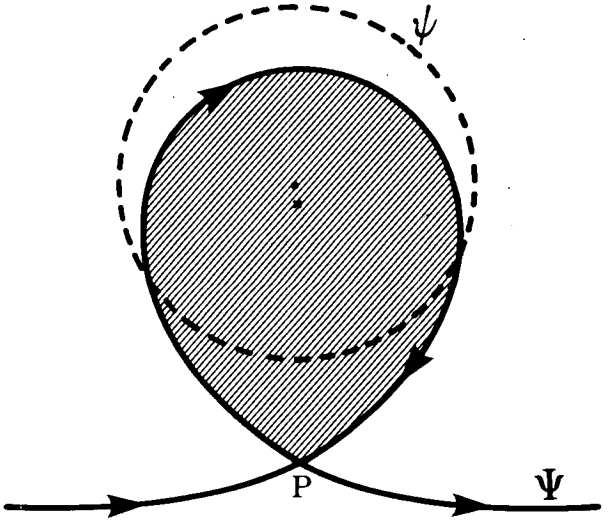

FIG. 1. A plot of the instantaneous streamfunction ψ and the streamfunction in a moving coordinate frame Ψ for a kinematic model of an anticyclonic ring (derived from Flierl, 1981). The Eulerian center of the ring is shown as the upper dot and the Lagrangian center as the lower cross. The hatched area denotes the region of trapped fluid, which translates with the ring. The vortex is "open" to its surrounding environment at critical point P.

(north). Typically, this distance is on the order of several kilometers.

More recently, satellite-derived sea surface temperature and chlorophyll concentration data have been particularly helpful in monitoring the motion and surface expression of rings (Brown *et al.*, 1983). The problem facing satellite oceanographers studying rings is inferring dynamical processes, such as ring translation, based solely on surface measurements. The high correlation between the location of subsurface fronts and their surface expression suggests that trajectories from satellite-derived data should agree with those from hydrographic data (Maul and Hansen, 1972; Brown *et al.*, 1983).

The data sets used for ring trajectory analysis, isolines of isotherm depth from hydrographic data, satellite-derived frontal positions, and drifter tracks, are outwardly very different. In terms of the retrieval mechanisms used, however, they are quite similar. Each is an approximation of a particular contour in two-dimensional space, and, as such, involve position errors and a limited set of data points around a ring. The first problem addressed by this study, therefore, is how the center estimate of a poorly sampled curve can best be computed. Some results concerning ring sampling strategies based on ring simulations involving eddies with variable translation velocities, eccentricities and sizes are presented with the development of this problem. One of the immediate benefits of this approach is an expected error curve for center estimation as a function of eddy size and translation relative to the time required for surveying the feature. Thus, an investigator interested in establishing a coordinate system in a particular eddy can determine the error in placing the origin and subsequent positioning in that system on the basis of the parameters of the vortex and the chosen survey pattern.

The rest of the study is concerned with how well differing data sets can be integrated to form a history of eddy motion. As a part of this analysis, the validity of using satellite-derived data and drifter trajectories to estimate the center of mass of a Gulf Stream ring is assessed. Two satellite data sets are used, one the redigitization of the other, in an effort to evaluate the importance of streamers and their connection to operator bias in the digitization process. This part of the analysis will also demonstrate whether the location of subsurface fronts and their surface expression are sufficiently well correlated to permit dynamically relevant calculations based on surface measurements and if the approximation of the ring front by a closed conic section is a good one.

2. Ring center algorithms

In finding the center of mass of a system of particles, it is necessary to consider the weighted average of the mass of each particle. In vector notation each particle of mass m in a system of total mass M can be described by a position vector $\mathbf{r}$ in a particular reference frame, and the center of mass can be located by a position vector $\mathbf{r}_{cm}$. In equation form,

$$\mathbf{r}_{cm} = \frac{1}{M}\int \mathbf{r}\,dm. \tag{1}$$

Center of mass estimation involves approximating this integral. Different data sets might require different estimation techniques due to differences in sampling methodologies. For general usage a single algorithm is preferred over a host of estimators, so there is the additional challenge of producing an estimator that can be applied to any one data set with equal competency. Here all of the data sets provide information on the horizontal location of trajectories or isolines of properties in the area of the ring with maximum swirl velocity, i.e., the high velocity region.

It is the boundary of the high velocity region that is seen so readily in satellite imagery and used most frequently in ship surveys to delineate the radial extent of the feature. The reason limited coverage of the high velocity portion of a ring provides a reasonable center of mass estimate is shown in Fig. 2. The figure shows the distribution of the volume anomaly per unit radius of waters warmer than 10°C in Gulf Stream warm core ring 82-B. The curve is computed from the azimuthally averaged depth anomaly of the 10°C isotherm compared to the surrounding Slope Water reference. The data used consist of all available XBT and CTD data from three ships that surveyed warm core ring 82-B in April and early May, 1982. The data is composited into a mean radial section by taking out the translation of the feature using the

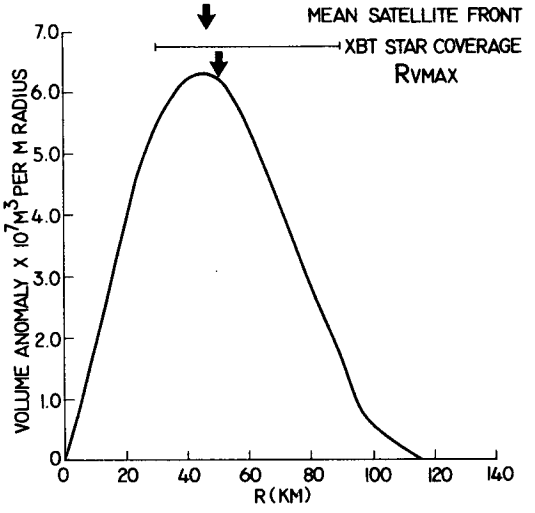

FIG. 2. Mean volume per unit radius as a function of distance from ring center R for the waters warmer than 10°C in warm core ring 82-B. The data used are from a composite of XBT and CTD casts from three ships in April and May 1984, in a cylindrical coordinate system moving with the ring.

techniques described here. The final volume anomaly per unit radius is then given by the integral

$$\text{Vol/unit } r = \int_0^{2\pi} [h(\theta, r) - h_r] r d\theta \qquad (2)$$

where h and h_r are the depths of the 10°C isotherm in the ring and the Slope Water reference, respectively.

The resulting volume per unit radius (Fig. 2) peaks near the radius of the velocity maximum (Rvmax). Individual synoptic surveys of this region of the ring cover a majority of the ring's total mass field as indicated by the XBT star surveys in Fig. 2. The thermal front around the ring also falls near the radius of maximum volume per unit radius. This front with its possible dynamic connection to the velocity maximum, therefore, provides a reasonable estimate of ring center of mass.

Center estimates are approximations of the mean position of a particular two-dimensional contour in space. The most straightforward calculation is simply the mean of all the retrieved positions of the sampled contour. The contour might be determined from interpolation of an isotherm at a particular depth or, equivalently, the digitization of a ring frontal boundary as seen in satellite thermal imagery. The former application is shown schematically in Fig. 3a as part of an XBT survey of a cold core ring. This estimator works well for cases with dense uniform sampling but gives large errors for uneven samples or samples with spatial gaps. It is, however, an estimation of the exact computation given in (1) when applied over the entire feature.

An alternative procedure is to choose a particular functional form for the idealized error and fit the observations to this function using least-squares analysis. Brown *et al.* (1983), for example, use a least-squares fit to a generalized quadratic equation for an ellipse for center estimation in a study of warm core ring kinematics using satellite-derived data. A generalized realization for this procedure is shown in Fig. 3b. Problems with this method include the assumption that a ring can be described by an ellipse, and that it is potentially unstable for partial sampling. The instability involves a switch of minor or major axis when there are large angular sections of missing data.

The center estimator concentrated on herein has the advantage of being fairly general while overcoming the elliptical fit routine's assumptions concerning ring

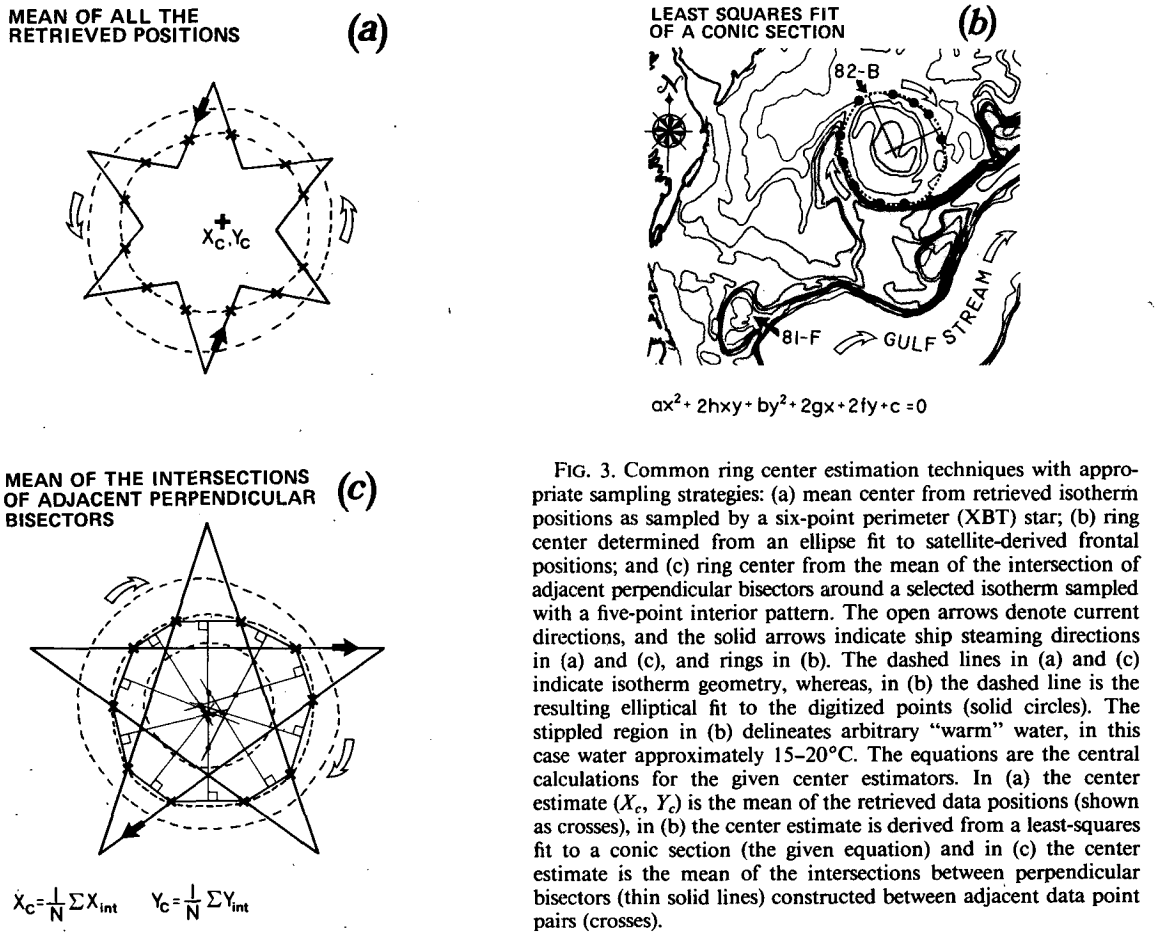

FIG. 3. Common ring center estimation techniques with appropriate sampling strategies: (a) mean center from retrieved isotherm positions as sampled by a six-point perimeter (XBT) star; (b) ring center determined from an ellipse fit to satellite-derived frontal positions; and (c) ring center from the mean of the intersection of adjacent perpendicular bisectors around a selected isotherm sampled with a five-point interior pattern. The open arrows denote current directions, and the solid arrows indicate ship steaming directions in (a) and (c), and rings in (b). The dashed lines in (a) and (c) indicate isotherm geometry, whereas, in (b) the dashed line is the resulting elliptical fit to the digitized points (solid circles). The stippled region in (b) delineates arbitrary "warm" water, in this case water approximately 15–20°C. The equations are the central calculations for the given center estimators. In (a) the center estimate (X_c, Y_c) is the mean of the retrieved data positions (shown as crosses), in (b) the center estimate is derived from a least-squares fit to a conic section (the given equation) and in (c) the center estimate is the mean of the intersections between perpendicular bisectors (thin solid lines) constructed between adjacent data point pairs (crosses).

shape and some of the difficulties the simple spatial averager has with sampling. This estimator is based on the intersection of adjacent perpendicular bisectors constructed between data point pairs around the desired contour. The center estimate is the mean of all the intersections between the adjacent perpendicular bisectors. An example of this calculation for a warm core ring surveyed with a five-point interior star is shown graphically in Fig. 3c.

The bisector method, of course, allows for other intersections besides those from adjacent data point pairs. Four different methodologies, each unique in its approach, can be devised to produce all possible bisector intersections. The procedure is to first categorize the chords that can be constructed between the data points as being either "minor" or "major", where minor chords join adjacent data point pairs and major chords join nonadjacent data point pairs. The intersections of the perpendicular bisectors between 1) adjacent minor chords (Fig. 3c), 2) nonadjacent minor chords, 3) minor and major chords and 4) only major chords, yield all possible intersections with no repetitions.

Due to eddy translation and ellipicity, misplacement of the survey pattern and interpolation errors, the data distribution is usually variable. With irregularly spaced data, minor chords can look like and, in terms of the methodology of the center estimator, act like major chords. To overcome this, a rejection criteria based on a spatial window or "box trap" is used to reject intersections that degrade, or have the potential for degrading, the center estimates. In the box trap, it is assumed the intersections of the perpendicular bisectors are normally distributed; thus, the center estimate is improved by rejecting intersections more than two standard deviations from the mean. The trap is then applied iteratively until the standard deviations subsequently begin to diverge; that is, the center estimate is calculated when the variance in the estimates is at a minimum. The procedure works well even with elliptical features because the intersections tend to cluster in two groups. Clustering produces a higher variance, which in turn leads to a large spatial window, which ensures that enough information is retained for the averaging of the intersections to be meaningful. A similar data control procedure is difficult to apply to the other center estimation methods and greatly enhances the ability of the chord estimator.

3. Simulations with the bisector methods

For circular features, there is no reason to expect any one of the bisector methods to outperform another. Rings are usually not completely circular, however, and it is likely that one of the methods is better suited for center estimation of ellipitical features, due to the differing geometry of various methods.

The bisector methods are evaluated using a model ring with variable ellipticity whose central thermocline level isotherm is described by a Gaussian function. Simulations involve translating and rotating rings. Ship sampling is acquired continuously using a variety of patterns as the ring translates out of the sampling area. To simulate the practice of surveying across the high velocity region, sampling is restricted near the depth of the inflection point of the Gaussian function.

The performance of each bisector method is based on how close the center and curvature estimates are to actual values. The tests show the superior bisector method to be the adjacent minor chord method, not only because it is able to provide center estimation for the entire range of sampling points used (up to 10 points), which the other methods are unable to do, but also because the quality of the estimate does not go down as the number of sampling points goes up. Consequently, any references to the bisector center estimator are, in fact, references to the adjacent minor chord method.

The perpendicular bisector method is then used in an analysis of ring sampling strategies. Three surveys are considered, all of them star-shaped: a six-point perimeter pattern (shown in Fig. 3a), a five-point interior pattern (shown in Fig. 3c) and a five-point perimeter pattern (outer outline of Fig. 3c). The star patterns were chosen because they provide synoptic coverage of the high velocity region and, hence, the majority of the ring's volume (Fig. 2). Both five-point patterns were used during the WCRE (Joyce, *et al.*, 1983), although the five-point interior pattern was used most often. The six-point pattern was the preferred sampling scheme in the Cyclonic Rings Experiment (Olson and Spence, 1978). From the vantage of center estimation, the superior pattern is the five-point perimeter pattern because of its greater synopticity, although the other two each have their unique advantages. For resolving azimuthal modes around the ring, for example, the six-point perimeter pattern is the best survey pattern, while, for ship drift and acoustic profiling applications, the five-point interior pattern is more appropriate.

Figure 4 is a nondimensional error analysis for the perpendicular bisector algorithm. For this simulation, a typical ring eccentricity (0.8) was chosen, the ring was not rotating and a five-point interior pattern was used to sample the ring over time. The curves delineate performance for the estimator in terms of error as a percentage of the radius to the velocity maximum (Rvmax) and are actually a result of compositing several simulations involving differing ring translation velocities (Co), survey lengths (Lsurv), ship speeds (Vs), and ring sizes (Rvmax). The figure shows the error in center estimation increases as survey placement worsens, $(X - Xo)/Rv$max increases and, as the synopticity of the pattern decreases, Ts/To increases. Historical Gulf Stream ring surveys are shown in Fig. 4, and, in most cases, the adjacent

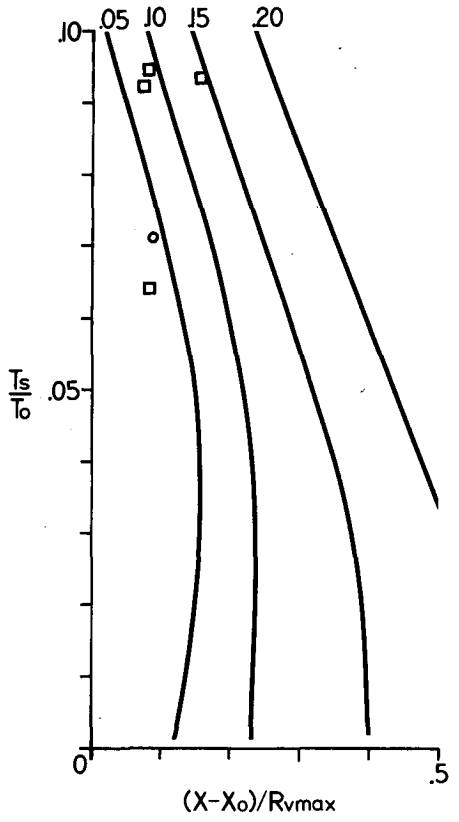

FIG. 4. The error in center estimation scaled by the radius to the velocity maximum as a function of survey positioning, $(X - Xo)/Rv\text{max}$, and synopticity, $Ts/To = (Co/Rv\text{max})/(Vs/L\text{surv})$; that is, the ratio of survey period (Ts) to ring translation period (To). $X - Xo$ is the offset in survey center with respect to ring center (Xo), $Rv\text{max}$ is the radius to the velocity maximum for the ring, Co is the translation speed of the ring, Vs is the velocity of the surveying vessel and $L\text{surv}$ is the length of the survey pattern. As a comparison to actual sampling patterns, an error estimate for a six-point star from the Cyclonic Rings Experiment is shown as a circle while several error estimates for Warm Core Rings five-point stars are shown as squares.

minor chord method is capable of center estimation to within 10% of the radius to the velocity maximum (approximately ±5 km for Gulf Stream rings).

4. Ring translation study

Three data sets from the second Warm Core Rings cruise in April 1982 are used for a ring translation study. The data sets used here are satellite-derived ring frontal positions, hydrographic measurements and drifter trajectories. This period was chosen because satellite coverage is extensive and relatively cloud free, ring translation is orderly and persistent, the ring is basically isolated (i.e., not interacting with the Gulf Stream, another ring or bottom topography) and ship coverage is extensive. Thus, the center algorithms are used under optimum conditions and linear analysis is applicable.

The satellite image data set was derived from the NOAA-7 satellite Advanced Very High Resolution Radiometer (AVHRR) instrument. The overall processing procedure used with these data is explained in detail by Brown and Evans (1982) and Brown *et al.* (1983). For the imagery used here, pixel location is to within ±1 km. The hydrographic data set was collected during a five-point interior XBT star (Fig. 3c) and an asterisk-shaped CTD survey. The drifter data were acquired from a LORAN-C surface drifter which telemetered and recorded its position internally twice an hour. The drifter was tied to the surface waters with a large "window shade" drogue situated at 100 m depth.

As a result of the optimization routines, the perpendicular bisector algorithm is not overly sensitive to partial sampling, although it does require some smoothing. For XBT and CTD data, a 10 km averaging window is used to remove multiple entries due to leg overlap in the star patterns. The effects of navigation noise in drifter data is reduced with a 2.5 km filter. To minimize digitization noise in the satellite-derived data, a 30 km averaging window is used. The choice of 30 km is based on minimizing the variance in the bisector-derived center estimates and maximizing the agreement between the perpendicular bisector and the elliptical fit routine.

Figure 5 is a plot of the satellite-derived trajectory for ring 82-B during a 13-day time interval in April 1982. The translation of the ring during the time interval is computed by regressing the ring center estimates versus time. Based on these computations, the ring was translating 5.6 cm s^{-1} toward the west and 0.8 cm s^{-1} toward the south. This is in close agreement with the classical picture of anticyclonic ring motion: westward translation with a small southerly component, and is of typical magnitude, ~5.0 cm s^{-1}. The regression curves were computed using

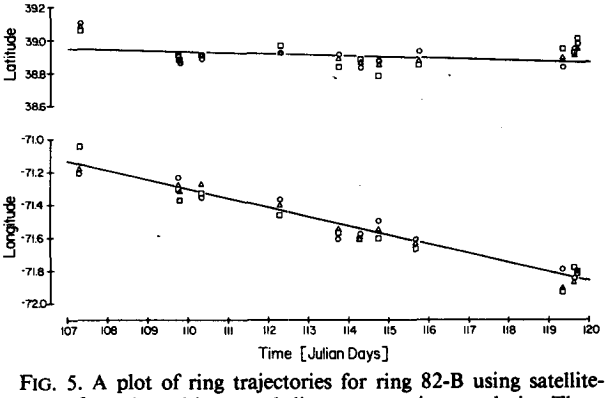

FIG. 5. A plot of ring trajectories for ring 82-B using satellite-derived frontal positions and linear regression analysis. Three different estimators are shown: the perpendicular bisector algorithm (circles), the elliptical fit routine (triangles) and a position averager (squares), but only the first two are used in the regression computations.

only the best estimators: the perpendicular bisector algorithm and the elliptical fit routine. T-test values for the individual trajectories indicate the curves are significant at the 95% level.

Predictably, the mean center estimator is not as reliable as the other estimators. If all three estimators are intercompared, the root-mean-square (rms) of the linear regression for the mean center estimator is 2 km above either of the other two estimators, and the significance of the regression is inferior, particularly in the latitude estimates. A comparison between the perpendicular bisector algorithm and the elliptical fit routine is more favorable, with the rms of the fits at the 5 km noise level of the calculation. The shape bias in the elliptical fit routine, then, is minimal, at least for the conditions considered. Under less optimal conditions, however, the perpendicular bisector algorithm would probably outperform the elliptical fit routine, because it is less sensitive to partial sampling.

Figure 6 is a plot of center estimates from XBT and CTD data for the period of interest. The center estimates are from the bisector algorithm only and are seen to span almost the entire time interval. Ring translation based on the XBT/CTD data is approximately 6.5 cm s^{-1} to the west and 1.3 cm s^{-1} to the south, which is only slightly higher than the previous satellite-derived velocities. As can be seen in the figure, the satellite-derived trajectory is south and west of the XBT/CTD trajectory, although the two converge as day 119 is approached. From day 110 to day 119, the difference between the satellite and XBT/CTD trajectory decreases from 9.5 to 0.0 km west in longitude, and from 6.7 to 1.1 km south in latitude. Center estimates from a LORAN-C drifter deployed from day 113 to day 118 show a similar behavior: they are south of the XBT/CTD trajectory (11.2 km on day 113) and only slightly west of it, with the exception of one point, but converge toward

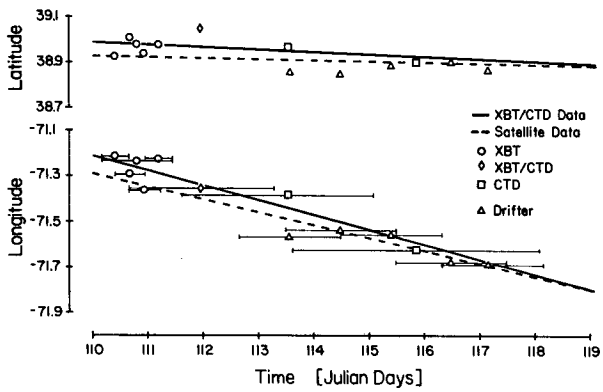

FIG. 6. A diagram comparing ring trajectories for ring 82-B from XBT/CTD data (solid line) with the satellite-derived trajectory determined earlier (dashed line). The thin solid lines denote the time period over which the data were collected for each center estimate.

it as day 119 is approached. Curiously, day 119 marks the beginning of a topographic interaction in which the ring is basically stationary.

If the hydrographic surveys are presumed sufficiently synoptic to permit the center estimates from XBT and, to a lesser degree, CTD stars to form an Eulerian representation of ring center motion, some kinematic comparisons concerning the data can be made. The kinematic arguments presented earlier and summarized in Fig. 1, indicate drifter-derived center estimates are positioned as expected; that is, they are displaced to the south of the center of mass trajectory during periods of ring translation, but are coincident with it during periods of no motion. The satellite-derived trajectory also exhibits this displacement in latitude, which suggests that the satellite data is more Lagrangian than Eulerian in nature. The kinematic arguments, however, cannot explain the westerly displacement of the satellite trajectory with respect to the XBT/CTD trajectory. This is probably due to biasing in one of the data sets.

Before accepting and further exploring these conclusions concerning the satellite data, then, it is appropriate to investigate biasing in the data. The XBT/CTD data is an unlikely source of bias. The perpendicular algorithm is an unbiased estimator, and, based on the test simulations, the practice of using thermocline level isotherms and the optimizing routines minimize the possibility of biasing as a result of improper surveying. The digitization of the ring frontal boundaries from satellite imagery is subject to a variety of potential errors by the digitizing operator; frontal boundaries, for example, can be obscured by clouds or water vapor inhomogeneities. There is also a fair amount of variability in the ring edge as seen from space, especially on the eastern (western) edges of the ring where cold (warm) streamers are pulled around the ring; a warm streamer can be seen on the western edge of ring 82-B in Fig. 3b. These errors, of course, change in importance and severity from image to image. It is possible, therefore, that over a short time interval, agreement or disagreement between satellite-derived data and *in situ* data might be mostly incidental and, in part, operator generated.

The original satellite data set was generated as the data was acquired, i.e., in real time. There are several problems with real time analysis of satellite data. One of the most vexing problems is maintaining continuity from one image to the next over a period of a month or longer. Frequently, an image is best interpreted if the next several images are available for scrutiny. To allay questions concerning biasing in the satellite data, the ring boundary data set was redigitized using a different operator and a more rigorous and systematic approach. In the new data set, the benefits of hindsight and additional imagery were used to improve the continuity of center estimates from one

day to the next. This led to a number of images being digitized an additional time and, in some cases, rejected altogether.

The effect of the redigitization is a slight overall improvement in the agreement between the satellite-derived data and the *in situ* measurements: on day 107 the new satellite trajectory is 6.0 km west and 7.8 km south of the XBT/CTD trajectory compared to 9.5 km west and 6.7 km south previously; on day 119 it is 0.9 km east and 1.1 km north compared to 0.0 km west and 1.1 km south before. These new values are not significantly above the noise level of the center estimates to indicate any real difference between the two satellite-derived trajectories, nor do they appreciably modify the kinematic arguments put forth earlier. The satellite trajectory is still south of the XBT/CTD trajectory. The greatest change between the two digitizations was in the longitudinal estimates, which points to the importance of the streamer field in regard to ring delineation and boundary interpretation.

5. Conclusions

The purpose of this study was to evaluate center estimation techniques for mesoscale eddies, and then to use the best estimators to investigate how well differing data sets (collected as part of an investigation of a Gulf Stream warm core ring) could be integrated to form a history of eddy motion. Three data sets were used for the time series: a drifter or Lagrangian data set, a hydrographic or Eulerian data set and a satellite-derived data set. Two objectives of the analysis were to determine the nature of the satellite-derived data set—Eulerian or Lagrangian—and to determine if sea surface temperature fronts are sufficiently well correlated with subsurface fronts to permit dynamically relevant calculations based on surface measurements.

Three center estimators were presented, each of which used a different estimation technique: one used the mean of the retrieved data positions, another, a least-squares fit of the data to a conic section and the third, the intersection of perpendicular bisectors constructed between adjacent data point pairs. Of these, the elliptical fit routine is the only biased estimator, since it assumes that the ring frontal boundary can be described by a conic section. A satellite-derived data set was used to evaluate the three estimators. The comparisons showed the superior estimators to be the perpendicular bisector algorithm and the elliptical fit routine. For the conditions considered, the two performed comparably. The shape bias in the elliptical fit routine, then, is minimal.

The XBT and CTD data were used to calculate the trajectory of the center of mass of the ring, which was compared to the trajectory based on the satellite-derived data. The two were seen to differ while the ring was translating but converged as it slowed due to a topographic interaction. This was also true for a Lagrangian trajectory computed from a LORAN-C buoy launched during the same time frame. The differences were seen to be in agreement with Flierl's (1981) kinematic model of rings. There was some concern, however, that the differences between the satellite-derived trajectory and the center of mass trajectory might be a result of biasing in the former due to streamer contamination. This led to the satellite-derived data set being redigitized by a different operator using a more rigorous and systematic approach. The new satellite trajectory compared slightly more favorably with the center of mass trajectory, but the satellite-derived estimates were still south of the XBT/CTD trajectory.

The pattern of separation during translation and coincidence during a period of no motion, suggests, following the arguments of Flierl (1981), that the satellite-derived ring positions are more Lagrangian than Eulerian in nature; that is, the surface feature in the ring is essentially a passive tracer pattern trapped in the swirl pattern set up by the thermocline depression. The consequences of this statement are far reaching and raise some interesting questions concerning the nature of the warm surface expression of the ring as seen from space. For instance, due to the close relationship between the ring boundary and the streamer field, it also suggests that streamers are passive elements, at least in the vicinity of the ring boundary.

Although the satellite trajectory was consistently south of the XBT/CTD trajectory, the difference between the two was near the noise level of the calculation. And just as importantly, the trajectories derived from the two separate satellite digitizations agreed to within the same level. To within approximately the error of the center estimates, then, satellite-derived data can be used to approximate the center of mass trajectory of a ring as determined by hydrographic surveys.

The perpendicular bisector algorithm was also used in conjunction with a Gaussian ring model and a star-shaped survey pattern to produce an expected error curve as a function of pattern synopticity and initial survey placement. For most survey circumstances involving typical rings, center estimation was usually possible to within ±5 km. This was shown to be the case for XBT surveys during the Cyclonic Rings and the Warm Core Rings Experiments. This, combined with the fact that satellite-derived data can be used to approximate the center of mass of a ring, suggests a detailed history of the motion and configuration of an eddy's mass field should be possible if satellite and hydrographic data are combined using the methods presented in this study. This is precisely what has been done with the entire Warm Core Rings data set. Positioning for the time series is reproducible to within 5 to 7 km and has been adopted by most

of the investigators in that program for plotting much of the biological, chemical and physical data.

Acknowledgments. The authors are part of a remote sensing group at the University of Miami's Rosenstiel School of Marine and Atmospheric Science (RSMAS). Without the willing participation of their fellow team members, much of what was presented would not have been possible. In particular, the authors are indebted to Robert Evans, Otis Brown and Jim Brown. Robert Evans and Otis Brown supplied the satellite time series for ring 82-B. Jim Brown was responsible for the development of the elliptical fit routine and the real time data analysis, although it was Robert Evans who redigitized the entire ring trajectory data set. The hydrographic data were collected under the guidance of Terry Joyce (WHOI), and the LORAN-C drifter was developed by Kevin Leaman (RSMAS). This work was funded by the National Science Foundation under Grants OCE8018736 and OCE8016991. The remote sensing facility of RSMAS is supported through grants to Otis Brown and Robert Evans from the Office of Naval Research, The National Aeronautics and Space Administration, and the National Science Foundation under Grants N00014-80-C-0042, NAGW-273 and OCE8016991, respectively.

REFERENCES

Brown, O. B., and R. H. Evans, 1982: Satellite visible and infrared remote sensing: A status report. *Nav. Res. Rev.*, **34,** 7–25.

——, D. B. Olson, J. W. Brown and R. H. Evans, 1983: Satellite infrared observations of warm core ring kinematics. *Aust. J. Mar. Freshwater Res.*, **34,** 535–545.

Chan, J. C. L., and W. M. Gray, 1982: Tropical cyclone movement and surrounding flow relationships. *Mon. Wea. Rev.*, **110,** 1354–1374.

Elliott, B. A., 1982: Anticyclonic rings in the Gulf of Mexico. *J. Phys. Oceanogr.*, **12,** 1292–1309.

——, and T. B. Sanford, 1983: The subthermocline lens D1. Part 1: Description of the water properties and velocity profiles. *J. Phys. Oceanogr.* (to be published).

Flierl, G. R., 1981: Particle motions in large-amplitude wave fields. *Geophys. Astrophys. Fluid Dyn.*, **18,** 39–74.

Henrick, R. F., M. J. Jacobson, W. L. Siegmann and R. L. Charnell, 1979: Use of analytical modeling and limited data for prediction of mesoscale eddy properties. *J. Phys. Oceanogr.*, **9,** 65–78.

Joyce, T., R. Backus, K. Baker., P. Blackwelder, O. Brown, R. Evans, G. Fryxell, D. Mountain, D. Olson, R. Schlitz, R. Schmitt, P. Smith, R. Smith and P. Wiebe, 1983: Rapid evolution of a Gulf Stream warm core ring. *Nature,* **308,** 837–840.

Maul, G. A., and D. V. Hansen, 1972: An observation of the Gulf Stream surface front structure by ship, aircraft, and satellite. *Remote Sens. Environ,* **2,** 109–116.

McDowell, S. E., and H. T. Rossby, 1978: Mediterranean water: an intense mesoscale eddy off the Bahamas. *Science,* **202:** 1085–1087.

Olson, D. B., 1980: The physical oceanography of two rings observed by the cyclonic ring experiment. Part II: Dynamics. *J. Phys. Oceanogr.*, **10,** 514–528.

Richardson, P. L., 1980: Gulf Stream ring trajectories. *J. Phys. Oceanogr.*, **10,** 90–104.

Ring Group (R. H. Backus, G. R. Flierl, D. R. Kester, D. B. Olson, P. L. Richardson, A. C. Vastano, P. H. Wiebe and J. H. Wormuth), 1981: Gulf Stream cold-core rings: their physics, chemistry, and biology. *Science,* **212,** 1091–1100.

Riser, S. C., W. B. Owens, H. T. Rossby and C. C. Ebbesmeyer, 1983: The structure, dynamics and origin of a small-scale lens of water in the western North Atlantic thermocline. *J. Phys. Oceanogr.* (to be published).

Smith, D. C. IV, and R. O. Reid, 1982: A numerical study of nonfrictional decay of mesoscale eddies. *J. Phys. Oceanogr.*, **12,** 244–255.

Willoughby, H. E., and M. B. Chelmow, 1982: Objective determination of hurricane tracks from aircraft observations. *Mon. Wea. Rev.*, **110,** 1298–1305.